The B[e] Phenomenon: Forty Years of Studies
ASP Conference Series, Vol. 508
A. Miroshnichenko, S. Zharikov, D. Korčáková, and M. Wolf, eds.

Clumping in Massive Star Winds and Its Possible Connection to the B[e] Phenomenon

B. Kubátová,[1,2] J. Kubát,[1] W.-R. Hamann,[3] and L. Oskinova[3]

[1]*Astronomický ústav AV ČR, Fričova 298, 251 65 Ondřejov, Czech Republic*

[2]*Matematički institut SANU, Kneza Mikhaila 36, 11001 Beograd, Serbia*

[3]*Institut für Physik und Astronomie, Universität Potsdam, Karl-Liebknecht-Str. 24/25, D-14476 Potsdam, Germany*

Abstract. It has been observationally established that winds of hot massive stars have highly variable characteristics. The variability evident in the winds is believed to be caused by structures on a broad range of spatial scales. Small-scale structures (clumping) in stellar winds of hot stars are possible consequence of an instability appearing in their radiation hydrodynamics. To understand how clumping may influence calculation of theoretical spectra, different clumping properties and their 3D nature have to be taken into account. Properties of clumping have been examined using our 3D radiative transfer calculations. Effects of clumping for the case of the B[e] phenomenon are discussed.

1. Introduction

Hot massive stars with winds are stellar objects predominantly of the O or WR spectral type that have strong line driven stellar winds. These stars are very luminous ($L > 10^{5.3} L_\odot$) and massive ($M \sim 10 - 50 M_\odot$). Effective temperatures of these stars are mostly above 30 kK. Although their lifetimes may be rather short ($\sim 10^6$ years) and they form only a small fraction of the stellar population, they dominate the light from galaxies. Some of these stars may overlap with stars with the B[e] phenomenon, mainly with the subgroup of B[e] supergiants.

The massive star wind mass-loss rates $\dot{M}$ are up to $10^{-6}\ M_\odot\ \mathrm{yr}^{-1}$ and wind terminal velocities v_∞ are up to $\sim 3000\,\mathrm{km\,s}^{-1}$. The outflow is accelerated by radiation. The largest part of the radiation force comes from photon scattering on lines of metals, while the force due to scattering on hydrogen and helium atoms is negligible. This momentum gained by metals is transferred to the rest of the wind by Coulomb collisions (for a review see, e.g., Krtička & Kubát 2007).

Determination of $\dot{M}$ and v_∞ is an important task in the analysis of massive stars. While measurement of the wind terminal velocity is quite straightforward using lines with the saturated P Cygni profile (mostly in the ultraviolet spectral region), determination of mass-loss rates is more subtle. No direct measurement is possible; the mass-loss rate is determined indirectly from atmosphere and wind models. Naturally, the theoretical flux prediction should fit the observation at all wavelengths. In other words, different parts of the spectrum should give the same results. However, Fullerton

et al. (2006) described discrepancy in the determination of mass-loss rates using different spectral regions. Mass-loss rates determined by fitting the P v line profiles differs from other determinations (Hα, radio). This discrepancy can be explained by using the assumption of a clumped wind (Šurlan et al. 2013).

2. Clumping in Massive Star Winds

Observational evidence of clumping. Although the massive star wind clumping can not be observed directly, it is possible to deduce the existence of clumps from line profile variability (e.g., Eversberg et al. 1998; Lépine & Moffat 1999; Markova et al. 2005). Indirectly, the presence of clumping is supported by X-ray observations (Oskinova et al. 2004). Additional evidence of wind clumping comes from observing flares in high-mass X-ray binaries with supergiants as their primaries (e.g., Fürst et al. 2010, for Vela X-1).

Supposed origin of clumping. Clumping in massive star winds is generally believed to originate from the radiative-acoustic instability (also known as the line deshadowing instability – LDI) inherent to the line-driving force (Owocki, Castor, & Rybicki 1988, see also the review by Sundqvist et al. 2012). However, other clumping mechanisms, such as adiabatic fluctuations (Chiueh 1997), subphotospheric convection (Cantiello et al. 2009), or some other hydrodynamic instability cannot be excluded a priori. Several mechanisms might play a role at the same time.

2.1. Description of Clumping

The lack of knowledge of the clump origin justifies the use of free parameters for description of clumping. Free parameters were already used for the description of condenstation in a nebula (Osterbrock & Flather 1959) before higher resolution observations became possible. Free parameters (filling factors) describing inhomogeneities (blobs) in the stellar wind were also used to describe the sources of wind X-ray radiation by Lucy & White (1980).

2.1.1. Microclumping

Abbott et al. (1981) used a two-component description of a clumped stellar wind containing high (ρ_H) and low (ρ_L) densities (clumps and interclump gas, respectively). This assumption is more often used in a simplified way additionally assuming $\rho_L = 0$, which means that all matter is present only in clumps and the space between them is void ("clumps in vacuum"). Adding additional assumption to the two-component description that *all* clumps are optically thin we arrive at the clumping model now referred to as the *microclumping* (Hamann & Koesterke 1998; Oskinova et al. 2007). This clumping model can be easily incorporated to 1-D NLTE wind model codes (e.g., PoWR, Hamann & Gräfener 2004, or CMFGEN, Hillier & Miller 1999).

Adjustable parameters for void interclump medium. Basic properties of clumps can be accounted for by a single parameter, which may be a *(volume) filling factor* f defined as a fractional volume occupied by clumps $V_{\rm cl}$ divided by the wind volume $V_{\rm w}$,

$$f = \frac{V_{\rm cl}}{V_{\rm w}}. \tag{1}$$

Alternatively, the ratio of density inside clumps $\rho_{\rm cl}$ (= ρ_H) versus the local mean density $\langle\rho_{\rm w}\rangle$,

$$D = \frac{\rho_{\rm cl}}{\langle\rho_{\rm w}\rangle} = \frac{1}{f}, \tag{2}$$

can be used. The quantity D is usually referred to as the *clumping factor*. Then the opacity and emissivity of a clumped medium can be expressed as

$$\chi_{\rm cl} = f\chi(D\rho_{\rm w}), \qquad \eta_{\rm cl} = f\eta(D\rho_{\rm w}), \tag{3}$$

respectively. The volume occupied by absorbing material is f times smaller, while the density inside clumps is D times larger. If all clumps are optically thin (microclumping), the resulting opacity depends on how particular processes are linked with density. For processes depending linearly on density, the average opacity of a clumped medium will be the same as for an unclumped medium, since $D = 1/f$. However, if the opacity depends on density squared, the average opacity in a clumped medium is D times larger. This holds, for instance, for recombination processes and thus for emission lines like Hα that are fed by the recombination cascade.

The influence of the interclump medium can be described using an additional parameter d introduced in Šurlan et al. (2012) as

$$d = \frac{\rho_{\rm ic}}{\rho_{\rm w}}, \tag{4}$$

where $\rho_{\rm ic}$ (= ρ_L) is the density of the medium between clumps. Hydrodynamical simulations (see Owocki et al. 1988) suggest that D should not be the same throughout the wind. To mimic this, Hillier & Miller (1999) introduced a depth dependent formula for the filling factor,

$$f(r) = f_\infty + (1 - f_\infty)\exp\left(-\frac{v(r)}{v_{\rm cl}}\right), \tag{5}$$

where f_∞ corresponds to f from Eq. (1) and $v_{\rm cl}$ is the location in the wind where clumping becomes important.

2.1.2. Macroclumping (porosity)

On the other hand, it is natural to expect that not all clumps are optically thin at all frequencies. However, this generalization introduces significant changes to resulting opacity. An optically thick clump means that it is not transparent, and all opacity coming from matter behind it is effectively lost since almost no radiation can reach it. As a result the total opacity may be reduced. Its quantitative estimates can hardly be done for 1-D radiation transfer (see Oskinova et al. 2004, who used the concept of "effective opacities"). It is necessary to take the full 3-D nature of the problem into account.

For a description of macroclumping we need more parameters. In addition to the ones used in the microclumping approach, D (Eq. 2) and d (Eq. 4), we have to introduce a parameter denoted as L_0. This parameter corresponds to the average separation between clumps (see Oskinova et al. 2007) and determines the total number of clumps in the wind. As another additional parameter describing the clump distribution we can introduce the onset of clumping $r_{\rm cl}$, which takes into account the results of 1-D hydrodynamical simulations that instabilities start around the wind critical point and continue downstream of the wind. This quantity corresponds to $v_{\rm cl}$ in Eq. (5). Using these parameters (D, d, L_0, $r_{\rm cl}$), the clump distribution can be calculated using the Monte Carlo

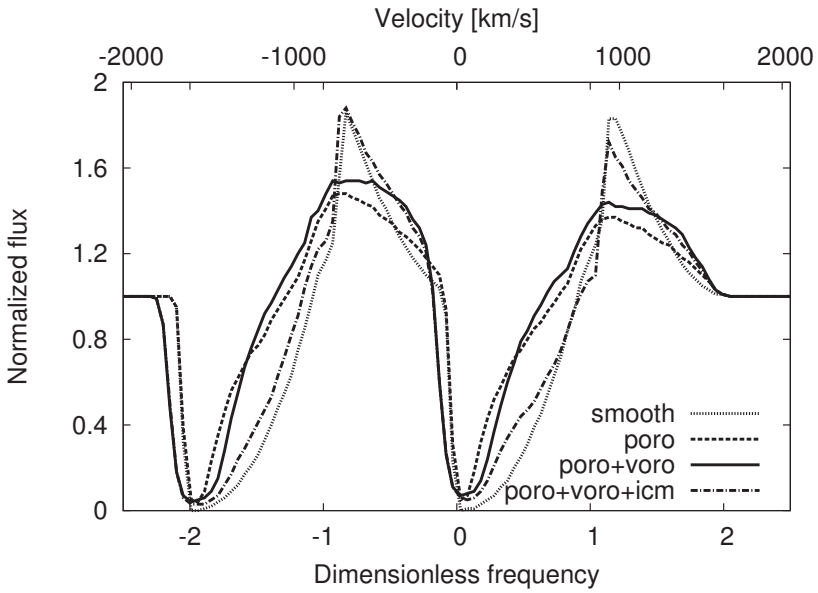

Figure 1. Effects of porosity and vorosity on P v line profile after Šurlan et al. (2012). The curve labeled "smooth" shows the line profile for a wind without clumps, "poro" shows the effect of macroclumping (porosity), "poro+voro" describes the profile assuming additionally the vorosity, "poro+voro+icm" shows the common effect of porosity, vorosity, and interclump medium together.

method. An additional free parameter $v_{\rm dis}$ can be used to describe the inhomogeneous velocity field ("vorosity").

Radiation transfer in clumped wind is then solved for a given clump distribution using a Monte Carlo method. The effects of macroclumping is demonstrated in Figure 1. For a detailed description of the Monte Carlo radiative transfer solution see Šurlan et al. (2012).

3. The P v Problem in Massive Star Winds

The resonance line of P v at 1118 and 1128 Å (transition $3s\,^2\mathrm{S}_{1/2} \leftrightarrow 3p\,^2\mathrm{P}^{\mathrm{o}}_{1/2,3/2}$) shows disagreement between theoretical and observed profiles (the latter are weaker), although other main spectral features are described well by theoretical profiles. It is possible to explain them by lowering the total abundance of phosphorus, as was attempted by Bouret et al. (2012). However, there is no reason for lower phosphorus abundance coming from the stellar evolution theory. The XUV radiation is able to change the ionization balance of phosphorus and lower the P v ionization fraction. This would not need to change the total phosphorus abundance. However, as pointed out by Krtička & Kubát (2012), the XUV radiation also affects other ions including those accelerating the wind. This would cause lowering the accelerating force and, consequently, changing the wind mass-loss rate and terminal velocity. This implies that lowering the phosphorus abundance is not a solution of the P v problem. Weaker profiles of P v resonance lines can be explained by macroclumping, as shown in Fig. 2 for the case of the star λ Cep.

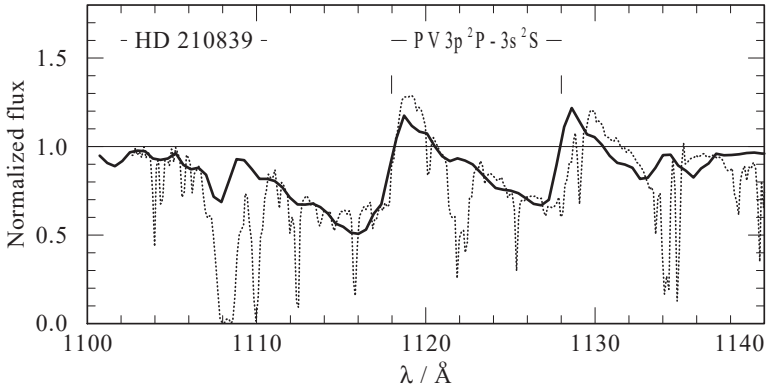

Figure 2. Fit of the P v resonance line profiles for λ Cep using clumping parameters $D = 10$, $d = 0.15$, $L_0 = 0.5$, $v_{\rm dis} = 0.01$ (after Šurlan et al. 2013).

4. Long Wavelength Radiation with Clumping

For microclumping, clumps are optically thin and the free-free emission formula by Panagia & Felli (1975) and Wright & Barlow (1975) can be used there. However, the flux $F_{\rm cl}$ for a clumped wind with an interclump medium changes as (Abbott et al. 1981)

$$F_{\rm cl}(\nu) = \left(\frac{f + (1-f)x^2}{\left[f + x(1-f) \right]^2} \right)^{\frac{2}{3}} F(\nu), \tag{6}$$

where $x = d/D$ and $F(\nu)$ is the flux from a smooth wind. For a void interclump medium ($x = 0$) this reduces to

$$F_{\rm cl}(\nu) = f^{-\frac{2}{3}} F(\nu). \tag{7}$$

With increasing clumping factor the radio radiation flux from the wind is stronger.

The situation with macroclumping is more complicated. It has been recently studied by Ignace (2016). The effect of clumping depends on clump shapes. While for clumps of the form of shell fragments the effect is similar to microclumping, for spherical clumps the differences depend on the filling factor. Significant differences appear only for extreme filling factors ($\sim 10^{-4}$). However, their existence is not supported by line formation calculations of Šurlan et al. (2013).

5. Clumping in B[e] Stars

Envelopes of B[e] stars are extremely large regions with specific conditions, which give rise to extremely strong emission in the Hα line and to appearance of forbidden emission lines. If clumping is present in B[e] star envelopes, it must be due to a different mechanism from that for other massive stars. Lower UV radiation (B[e] stars are cooler) also causes the radiation force to be weaker and, as a consequence, it is unclear whether it provides enough momentum for a strong wind. However, even for a weak wind the line-deshadowing instability exists. Real effects (if any) have to be tested by hydrodynamical simulations. Luckily (for the existence of clumping), there are alternative mechanisms potentially able to create instabilities and clumping, namely the

subphotospheric convection, and even common hydrodynamical instabilities may play a role. If clumping is present there, it might also influence the continuum radiation significantly and reduce the forbidden line emission.

6. Summary

There is a growing evidence that clumping is present in the massive star winds. Using macroclumping we are able to reproduce their wind spectra consistently, in contrast to a wind model with only microclumping. For massive stars, the presence of clumping is also supported by observational evidence. However, observational indications of clumping in B[e] stars are missing. Due to similar physical conditions in their envelopes, it is reasonable to expect that clumping is present in the envelopes of B[e] stars as well. If clumping is actually present in B[e] stars, it has to affect their emergent spectra.

Acknowledgments. GA ČR grants 14-02385S and 16-01116S.

References

Abbott, D. C., Bieging, J. H., & Churchwell, E. 1981, ApJ, 250, 645
Bouret, J. C., Hillier, D. J., Lanz, T., & Fullerton, A. W. 2012, A&A, 544, A67
Cantiello, M., Langer, N., Brott, I., de Koter, A., Shore, S. N., Vink, J. S., Voegler, A., Lennon, D. J., & Yoon, S. C. 2009, A&A, 499, 279
Chiueh, T. 1997, ApJ, 482, 179
Eversberg, T., Lépine, S., & Moffat, A. F. J. 1998, ApJ, 494, 799
Fullerton, A. W., Massa, D. L., & Prinja, R. K. 2006, ApJ, 637, 1025
Fürst, F., Kreykenbohm, I., Pottschmidt, K., Wilms, J., Hanke, M., Rothschild, R. E., Kretschmar, P., Schulz, N. S., Huenemoerder, D. P., Klochkov, D., & Staubert, R. 2010, A&A, 519, A37
Hamann, W. R., & Gräfener, G. 2004, A&A, 427, 697
Hamann, W. R., & Koesterke, L. 1998, A&A, 335, 1003
Hillier, D. J., & Miller, D. L. 1999, ApJ, 519, 354
Ignace, R. 2016, MNRAS, 457, 4123
Krtička, J., & Kubát, J. 2007, ASPC, 361, 153
— 2012, MNRAS, 427, 84
Lépine, S., & Moffat, A. F. J. 1999, ApJ, 514, 909
Lucy, L. B., & White, R. L. 1980, ApJ, 241, 300
Markova, N., Puls, J., Scuderi, S., & Markov, H. 2005, A&A, 440, 1133
Oskinova, L. M., Feldmeier, A., & Hamann, W. R. 2004, A&A, 422, 675
Oskinova, L. M., Hamann, W. R., & Feldmeier, A. 2007, A&A, 476, 1331
Osterbrock, D., & Flather, E. 1959, ApJ, 129, 26
Owocki, S. P., Castor, J. I., & Rybicki, G. B. 1988, ApJ, 335, 914
Panagia, N., & Felli, M. 1975, A&A, 39, 1
Sundqvist, J. O., Owocki, S. P., & Puls, J. 2012, ASP Conf. Ser., 465, 119
Šurlan, B., Hamann, W. R., Aret, A., Kubát, J., Oskinova, L. M., & Torres, A. F. 2013, A&A, 559, A130
Šurlan, B., Hamann, W. R., Kubát, J., Oskinova, L. M., & Feldmeier, A. 2012, A&A, 541, A37
Wright, A. E., & Barlow, M. J. 1975, MNRAS, 170, 41